Research Article

Hydraulic Erosion Rate of Reinforced Tailings: Laboratory Investigation and Prediction Model

Xuanyi Chen (ID),[1] **Xiaofei Jing** (ID),[1] **Hai Cai,**[2] **Yijun Wang,**[1] **and Luhua Ye**[1]

[1]*School of Safety Engineering, Chongqing University of Science and Technology, Chongqing 401331, China*
[2]*Sichuan Provincial Bureau of Geological and Mineral Exploration Geological Team 202, Sichuan 610000, China*

Correspondence should be addressed to Xuanyi Chen; 2584304676@qq.com and Xiaofei Jing; xfjing@cqust.edu.cn

Tailings dams are high-potential-energy dams built to store various ore tailings, and the overtopping failure caused by hydraulic erosion is one of the most common failure modes. The characteristics of hydraulic erosion of the reinforced tailings were studied by using the self-made erosion apparatus with four kinds of reinforcement spacing 2.5, 1.7, 1.3, and 1.0 cm, respectively. The test results show a positive correlation between the reinforcement spacing and erosion rate of tailings. Based on the sediment scouring theory, the scouring constant in the erosion rate formula is determined to be 0.056 mm/s; a prediction model for the hydraulic erosion rate of reinforced tailings is established by introducing the collapse coefficient into the results of the overflow test of reinforced tailings. This model can provide a reference for the prediction of overtopping-induced erosion failure of the reinforced tailings dam.

1. Introduction

Tailings dam is a sizeable high potential energy facility used to store the waste after beneficiation, and the primary process is to discharge the slurry precipitation into the tailings dam. However, the tailings dam is a dangerous source of artificial debris flow with high potential energy. Once the dam break occurs, the safety of downstream residents and facilities will be threatened. Tailings dam accidents frequently occurred in recent years, including dam liquefaction, overtopping erosion, and collapse, which has brought serious disaster to the life of downstream people [1–6]. At present, most researchers take unreinforced tailings dam as the research object, and there are few studies carried out on the erosion failure of the reinforced tailings dam. Sun et al. [7] proposed a failure evolution model of unreinforced tailings dam overtopping through the physical model test. Dang et al. [8] divided the dam failure evolution stages of the tailings dam during flood overtopping with different accumulation densities. Wang et al. [9] discussed the physical characteristics, mode, and development regularity of dam break in the process of water level rise through

the flood overtopping dam-break test of the tailings dam. Zhang et al. [10] used the self-made dam-break model test platform of a tailings dam to carry out the dam-break model test of the tailings dam with a similarity ratio of 1 : 100. The evolution of dam displacement, infiltration line, maximum velocity, and dam failure was also analyzed. It found that the collapse of the tailings dam first occurs at the foot of the slope, showing traceability failure. Some scholars [11, 12] studied the dam failure causes and dam failure evolution process of tailing dams under different rainfall conditions, as well as the causes of flood overtopping dam failure. None of the above researchers studied the overtopping of the reinforced tailing dams, failure analysis of tailings dam failure mode, failure mechanism and cause of dam failure, and reinforced tailings dam analysis of the impact of few scholars to study. Geosynthetics have been widely used in tailing dam engineering. Adding geogrid in tailings can effectively improve the shear strength of soil and reduce the erosion of water flow during flood overtopping. In the process of hydraulic erosion, the influence of reinforcement on tailings dam particles is worth studying [13, 14]. Jing [15] and Zhou [16] revealed that the increase of reinforcement density

could improve the mechanical strength of tailing dams by studying the effect of band density on the overtopping failure of the tailings dam, and the difference of the development model of the reinforced and unreinforced tailing dam breach is also analyzed. The interpretation of the influence of geogrid density on tailing dam failure provides the scientific basis for the research of tailing dam reinforcement.

At present, there have been studies on sediment incipient motion, sediment scouring, viscous sediment scouring, and overtopping failure of the reinforced tailings dam, but few researchers studied the multifactors coupling of the viscous tailings scouring and the geogrid. Overtopping failure is the leading cause of erosion damage of tailings dam. To predict the failure process of overtopping erosion of tailings dam, it is necessary to obtain the erosion rate, that is, the erosion height per unit area per unit time. In addition, it is also essential to establish semitheoretical or semiempirical formulas of the hydraulic erosion rate of tailings dam based on the formula of incipient motion velocity of the tailings dam, to analyze the force of cohesionless sediment particles under the action of water flow. Zhao et al. [17] analyzed the influence of microtopography on hydraulic erosion and its change during rainfall by comparing the smooth surface with the rough surface and analyzed the effect of the surface morphology on runoff and sediment transport. Briaud [18] measured the shear stress and erosion rate of water flow at different flow velocities through a self-developed erosion test device. Wang and Wu [19] introduced a new viewpoint of flow bed-moving force and analyzed the functional relationship between the fluctuation of near-bottom water flow. The results showed that the flow of bed-moving force and the fluctuation intensity of water flow is positively correlated. Kandiah [20] obtained the nonlinear relationship between the sediment erosion rate and the relative residual shear stress through the silt scouring test and established the formula of the sediment scouring rate by the dimensionless method. Researchers such as Zhang et al. [21], Osman and Thorne [22], Krone [23], and Sanford and Maa [24] established the erosion formula of cohesive sediment through the results of erosion tests. Different from Kandiah [20], Li et al. [25] obtained the nonlinear relationship between the sediment erosion rate and the relative residual shear stress through the silt erosion test. The physical and chemical properties index l was proposed according to the dimensionless method, and Li established the formula of sediment erosion rate.

In this paper, the self-made hydraulic erosion test device for reinforced tailings is used to carry out the erosion test of reinforced tailings dams. The erosion rate formula is established, referring to a similar idea in sediment research [26–34]. The erosion rate model of tailings dam with various reinforcement spacing is obtained by fitting the erosion constants and physicochemical indices in the formula with test data. Through the results of the overtopping failure test of the reinforced tailings dam, the collapse coefficient $K(d)$ is introduced to establish the formula of the hydraulic erosion rate of the reinforced tailings dam, which can provide a reference for the study of microscopic characteristics of hydraulic erosion damage of the reinforced tailings dam.

2. Experimental Method

2.1. Experimental Facilities. The experimental erosion facilities consist of a glass flume, a rectangular horizontal acrylic tube with the diameter of a sample hole of 5 cm under the bottom of the tube, sample tube, electromagnetic flowmeter, water pump, and overflow tank (as shown in Figure 1).

An aluminum alloy sample tube with an inner diameter of 5 cm is used as the sample tube. Then Vaseline is smeared on the inner wall of the tube to keep the degree of compaction constant when the sample is jacked up. The piston has good sealing performance and can be vertically reinforced in the sample tube. In order to reduce the hydraulic roughness, the horizontal tube made of organic glass is used for observation tests. And the horizontal tube size is 180 cm × 8 cm × 5 cm (length × width × height). The size of the water storage tank is 2 m × 0.6 m × 0.6 m (length × width × height). The circulating water supply power device adopts a water pump with a power of 1.5 kW and a flow rate of 40 m³/h. The high-resolution cameras (SONY, Beijing, China, resolution: 1920 × 1080/50p) are used as observation devices. Finally, the water level is kept constant through the overflow tank.

2.2. Materials and Experimental Procedures. The particle size, gradation, and compactness of silt will influence the constant scouring K of erosion. The tailings soil cover of a tailings pond in Yunnan is used in this test. And the particle size range of the tailings pond is 0.005~0.30 mm. The cumulative distribution curve of the particle size is shown in Figure 2. Next the raw tailings are sieved into four-particle size grades, which are 0~0.038 mm, 0.038~0.075 mm, 0.075~0.109 mm, and 0.109~0.27 mm. Then the tailings soil of the four-particle size grades is proportioned according to different quality percentage requirements. Finally, eight groups of tailings soil samples with different particle sizes are formed, shown in Table 1.

2.3. Test Method. The test is carried out on a reinforced tailings erosion device. The tailings with 15% water content were prepared according to the test requirements, and the reinforcement spacing is 2.5 cm, 1.7 cm, 1.3 cm, and 1.0 cm, respectively. The tube with a diameter of 2.5 cm is inserted into 1, 2, 3, and 4 layers glass fiber window screen [26] as reinforcement, respectively. The reinforcing geogrid specification is 1.5 mm × 1.5 mm aperture. As shown in Figure 3, before carrying out the erosion test, the quality and height of the test tailings samples are measured first.

2.3.1. Test Process. The detailed procedures of the erosion test of reinforced tailings are listed as follows:

① Using the lifting jack pushes the reinforced tailings in the sample tube into the horizontal tube for 1~3 mm as shown in Figure 4.

② Close the valve of the horizontal tube and slowly inject water into the horizontal tube until it is filled with water.
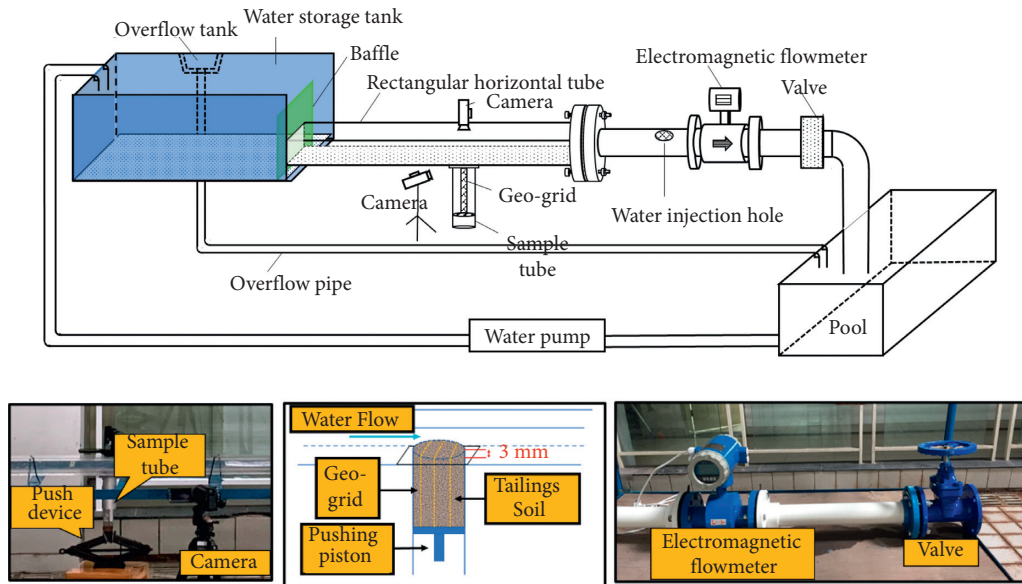
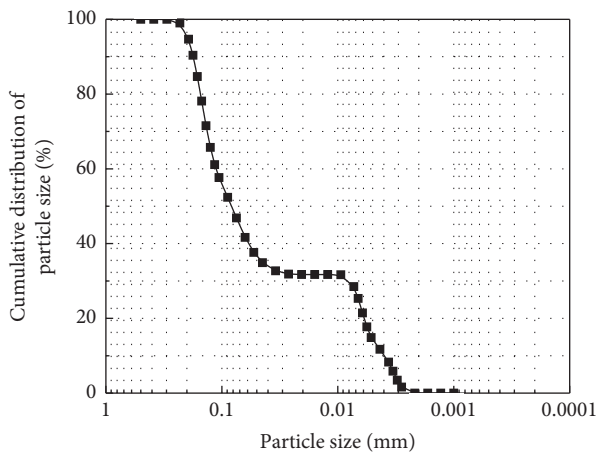Figure 1: Erosion apparatus to measure erodibility.

Figure 2: The cumulative size distribution curve of the tailings sample.

③ Open the valve, adjust the size of the valve to ensure that the flow velocity is greater than the incipient motion velocity of tailings.

④ Pull out the piston blocking the valve to start the erosion test. This method can reduce the erosion and damage of the sample as much as possible when the flow velocity increases.

⑤ The total erosion time of the reinforced tailings is 120 seconds.

2.3.2. Reading of Erosion Velocity. The erosion test needs to measure the average velocity of the water flow in a fixed erosion time, but not the instantaneous threshold incipient motion velocity test. Because the reading of the electromagnetic flowmeter fluctuates in the order of 0.01 m³/h, the average velocity calculated by the average flow rate is used as the erosion velocity. The flow rate is recorded by an electromagnetic flowmeter, and then the average flow rate is obtained by comparing the flow rate with the cross-sectional area of the horizontal tube.

2.3.3. Determination of Erosion Height. In the test process, the height of the reinforced tailings sample eroded in a fixed time was measured. When the valve knob reaches the correct position, the erosion test starts, and the erosion of the sample is recorded until the end of the fixed erosion time. The erosion height of the corroded reinforced tailings samples was measured at several positions, and the average value was adopted.

3. Results and Discussion

3.1. Test Phenomenon and Analysis. The tailings sample 4 and the reinforcement number of 2 (the reinforcement spacing is 1.7 cm) are taken as an example to show the phenomenon of the erosion test, as shown in Figure 5. The erosion test starts after the reinforced sample is pushed 2 mm into the horizontal tube, and the valve is opened with five and a half cycles (flow rate of 4.5 m³/h). As can be seen from Figure 5(a), the front end of the sample pushed into the horizontal tube is far away from the band, and there is no geogrid affecting the soil. The front end of tailings soil is first impacted by water flow and erodes quickly, just like that without reinforcement. With the continuous erosion of the water flow, the tailings in front of the band (the first side affected by the water flow) are gradually eroded completely, making the tailings level to the bottom of the horizontal tube. However, the tailings behind the second layer of the rear reinforcement are blocked by the reinforcement and gradually accumulated to form sand ridges, as shown in Figure 5(b). As the test continues, the tailings far behind the second layer of the reinforcement gradually increase. The sample area near the rear of the first layer of the geogrid is

TABLE 1: Proportioning of tailings samples.

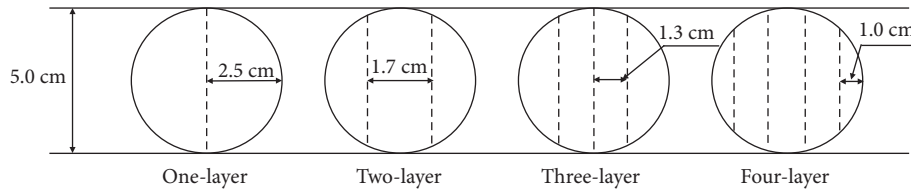| Tailings samples	Quality percentage of tailings with various particle sizes				Median diameter (mm)
	<400 mesh (<0.038 mm) (%)	400~200 mesh (0.038~0.075 mm) (%)	200~140 mesh (0.075~0.109 mm) (%)	140~50 mesh (0.109~0.27 mm) (%)	
1	50	30	20		0.0071
2	20	50	30		0.0426
3	30	20	50		0.0476
4	20	10	60	10	0.0487
5	10	10	20	60	0.0508
6	10	20	50	20	0.0826
7	20	50	10	20	0.0971
8	25	25	25	25	0.1536

FIGURE 3: Diagrams of different geogrid arrangements and reinforcement space.
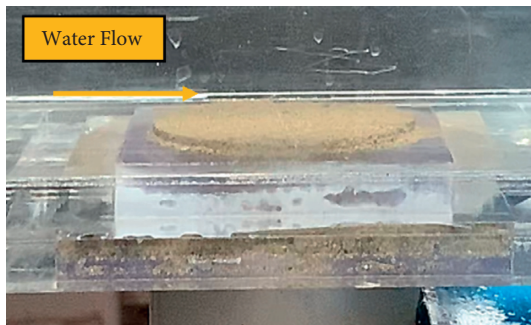

FIGURE 4: Schematic of sample pushing into a horizontal tube.

exposed in the flow, which forms a vortex and a deep concave in the flow, as shown in Figure 5(c). With the test continuing, a gradual increase occurs in the concave behind the first layer of reinforcement. The sand ridge behind the second layer of the geogrid also gradually increases and moves backward along the flow direction. At this time, the tailings near the front of the first layer are progressively eroded. Finally, with the increase of erosion time, the sand ridge formed behind the band is gradually eroded as well, as shown in Figure 5(d).

When the exposed length of the reinforced tailings is short, it is hard for the reinforced tailings to bend, which can be regarded as the situation of the local scour of the pier. Therefore, the erosion phenomenon of the reinforced tailings under hydraulic action can be explained by the local scour theory of piers. Therefore, the scouring phenomenon of reinforced tailings under hydraulic action can be explained by the local flushing mode of bridge piers studied by Briaud [18]. Due to the influence of water flow, the flow structure near the pier is divided into descending flow, horseshoe vortex, and wake vortex [27]. As shown in

Figure 6, in the erosion process, a part of the flow and the longitudinal reinforcement can be seen as the pier erosion, which makes the wake vortex behind the reinforcement cause tailings erosion. The tailings in front of the longitudinal reinforcement also erode the tailings due to the horseshoe vortex. In the other parts, descending flow is formed due to the influence of the transverse geogrid. After converging with the flow passing through the geogrid, a vortex is formed behind the geogrid. Therefore, the tailings behind the first layer of reinforcement is the most seriously eroded due to the combined action of two parts of water flow.

For the tailings samples with other reinforcement spacing, the erosion test process is the same as the above process. It can be seen from the erosion process that the reinforced tailings samples will not be eroded to the uniform horizontal height by water flow, but there are pits of varying degrees. Therefore, in the reinforced tailings erosion tests with 1, 2, 3, and 4 layers of reinforcement, the reinforcement spacing is 2.5, 1.7, 1.3, and 1.0 cm, respectively. The erosion height is measured at several positions of the final tailings sample and the average erosion height is taken; then, we use the fixed time to calculate the erosion rate.

3.2. Results and Analysis. In the erosion process, the quality, total thickness, flow rate (Q), erosion time (t), and erosion height (h) are measured, and the flow velocity and erosion rate of reinforced tailings are calculated. The erosion rate is shown in Tables 2–5.

Figure 7 shows the erosion rate of the tailings in the middle of the particle size range of 8 samples under different reinforcement spacing of 2.5, 1.7, 1.3, and 1.0 cm, respectively. It can be seen from Figure 7 that the reinforcement spacing has a noticeable effect on the erosion rate of tailings. With the increase of the reinforcement spacing, the erosion rate of the reinforced tailings increases; the test results show
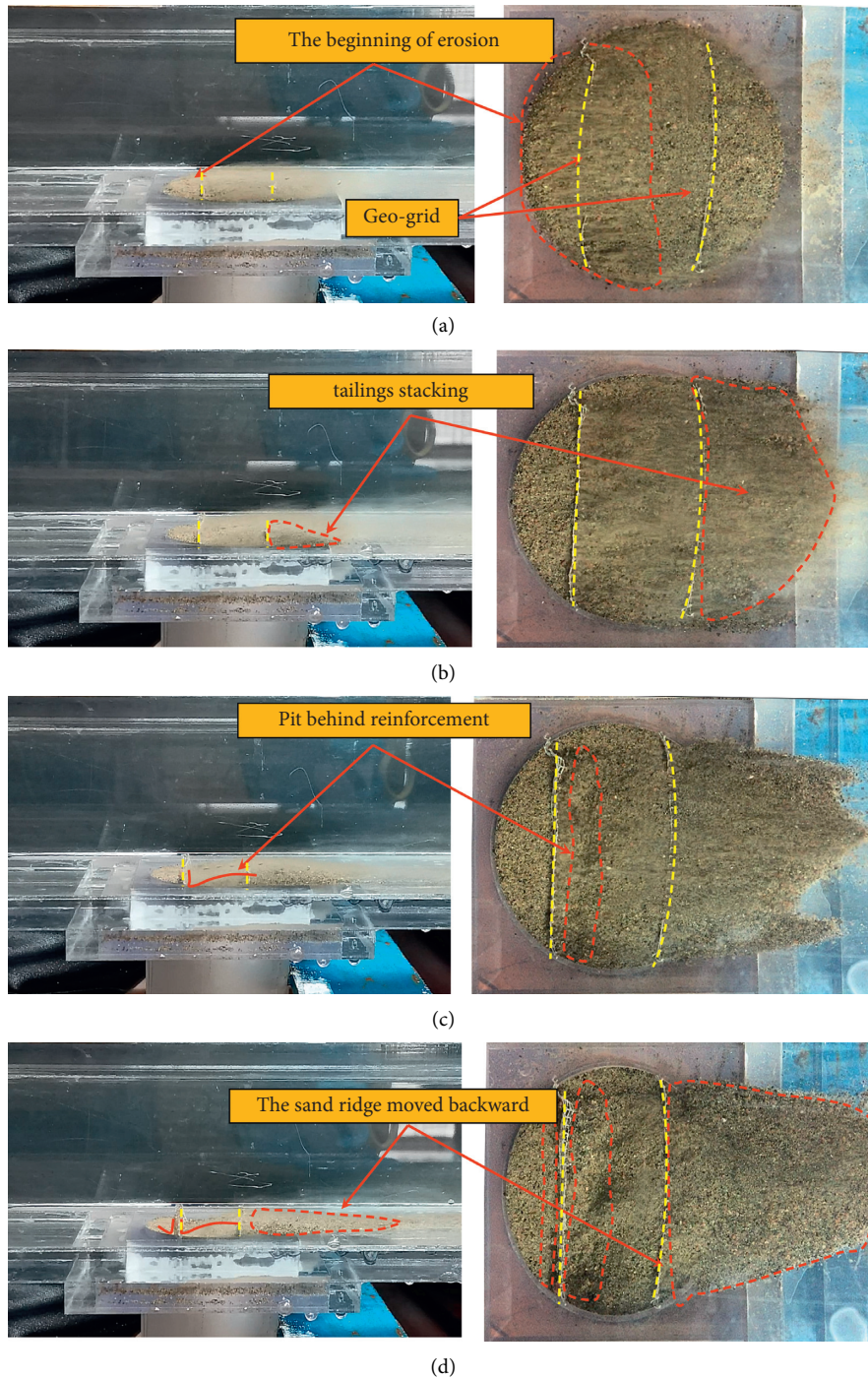
(a)

(b)

(c)

(d)

Figure 5: Tailings erosion phenomena with different geogrid spacing. (a) The front end of the sample begins to erode. (b) The front end of the sample is flushed, and the tailings behind the second layer of reinforcement are stacked. (c) Concavity of tailings behind the first layer of the band. (d) Backward movement of tailings ridge behind the second layer.

that when the reinforcement spacing is 1.0 cm, the corrosion rate of the reinforced tailings Sample 2 is 0.025 mm/s, while when the reinforcement spacing is 2.5 cm, the erosion rate of reinforced tailings is 0.058 mm/s. Therefore, it can be seen that the closer the reinforcements are, the smaller the erosion rate is. The main reason is that the existence of the reinforcement slows down the corrosion rate of the tailings sample. Based on the theory of quasicohesive reinforcement of geogrid, it can be concluded that the effect of adding of geogrid will increase the pseudocohesive force c_1 of tailings, which can enhance the antiscour performance of the sample. However, with the increase of the reinforcement spacing of reinforced tailings, the pseudocohesive force of geogrid decreases gradually. It is shown that the reinforcement range of the geogrid is limited when it is used in the tailings. Therefore, only the particles near the reinforcement will be
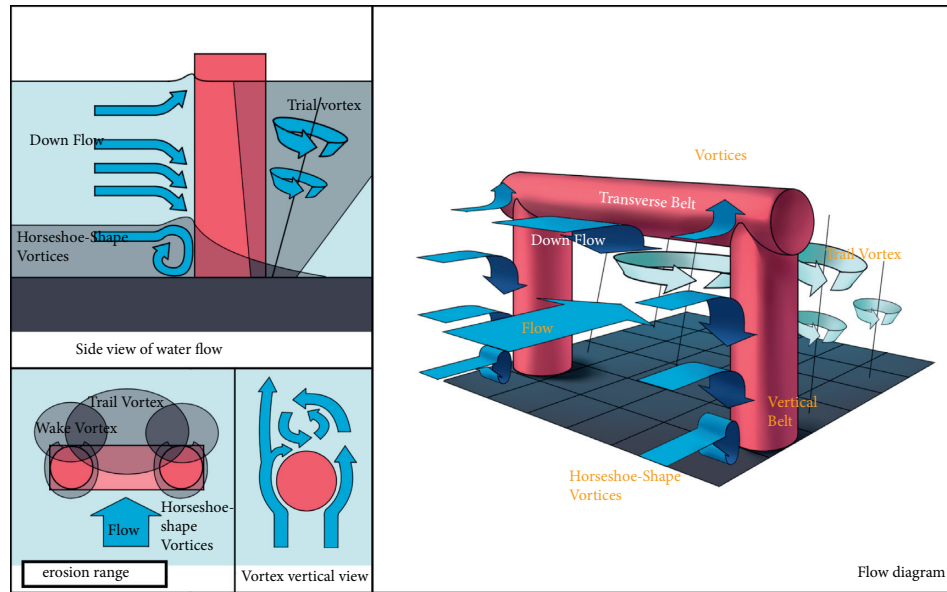
FIGURE 6: The flow structure at the geogrid.

TABLE 2: Experimental data of tailings erosion with the reinforcement spacing of 2.5 cm.

Geospacing d (cm)	Sample number	Flow rate Q (m³/h)	Flow velocity U(m/s)	Erosion time t (s)	Erosion height h (mm)	Erosion rate E (mm/s)
	1	12.1	0.840	120	7.4	0.062
	2	3.8	0.264	120	7.0	0.058
	3	3.8	0.264	120	5.8	0.048
2.5	4	3.8	0.264	120	8.0	0.067
	5	3.8	0.264	120	8.5	0.071
	6	3.8	0.264	120	9.0	0.075
	7	3.8	0.264	120	6.8	0.057
	8	3.8	0.264	120	6.5	0.054

TABLE 3: Experimental data of tailings erosion with the reinforcement spacing of 1.7 cm.

Geospacing d (cm)	Sample number	Flow rate Q (m³/h)	Flow velocity U (m/s)	Erosion time T (s)	Erosion height h (mm)	Erosion rate E (mm/s)
	1	12.1	0.840	120	6.2	0.052
	2	3.8	0.264	120	5.7	0.048
	3	3.8	0.264	120	5.0	0.042
1.7	4	3.8	0.264	120	6.3	0.053
	5	3.8	0.264	120	7.0	0.058
	6	3.8	0.264	120	6.5	0.054
	7	3.8	0.264	120	5.3	0.044
	8	3.8	0.264	120	5.2	0.043

TABLE 4: Experimental data of tailings erosion with the reinforcement spacing of 1.3 cm.

Geospacing d (cm)	Sample number	Flow rate Q (m³/h)	Flow velocity U (m/s)	Erosion time t (s)	Erosion height h (mm)	Erosion rate E (mm/s)
	1	12.1	0.840	120	4.7	0.039
	2	3.8	0.264	120	4.5	0.038
	3	3.8	0.264	120	3.7	0.031
1.3	4	3.8	0.264	120	5.0	0.042
	5	3.8	0.264	120	5.8	0.048
	6	3.8	0.264	120	6.0	0.050
	7	3.8	0.264	120	4.2	0.035
	8	3.8	0.264	120	4.0	0.033

TABLE 5: Experimental data of tailings erosion with the reinforcement spacing of 1.0 cm.

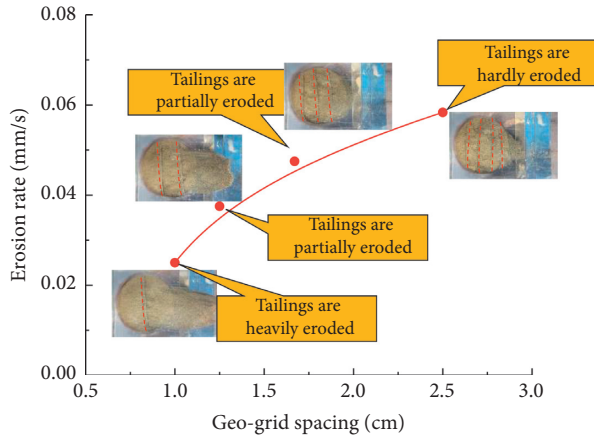| Geospacing d (cm)	Sample number	Flow rate Q (m^3/h)	Flow velocity U (m/s)	Erosion time t (s)	Erosion height h (mm)	Erosion rate E (mm/s)
	1	12.1	0.840	120	3.2	0.027
	2	3.8	0.264	120	3.0	0.025
	3	3.8	0.264	120	1.8	0.015
1.0	4	3.8	0.264	120	3.9	0.033
	5	3.8	0.264	120	4.5	0.038
	6	3.8	0.264	120	5.0	0.042
	7	3.8	0.264	120	2.8	0.023
	8	3.8	0.264	120	2.5	0.021

FIGURE 7: Relationship between erosion rate and geogrid spacing.

strengthened, with the antiscour performance improved. In summary, the reduction of the reinforcement spacing in tailings can improve the antiscouring ability, which reduces the water flow erosion on tailings and overtopping.

4. Prediction Model of Hydraulic Erosion Rate of Reinforced Tailings

4.1. Establishment of Erosion Rate Based on Erosion Test.
Liu [28] introduced the concept of geogrid coefficient $f(d)$ and established the calculation formula of incipient motion velocity of reinforced tailings particles. Then, through the test data of incipient motion velocity of reinforced tailings, the specific expression of geogrid coefficient $f(d)$ is fitted. Finally, the calculation formula of incipient motion velocity of tailings particle reinforcement is established. V_c' is shown in the formula:

$$V_c^{'} = \left(1 + e^{(-d/0.73)}\right) \cdot V_c, \tag{1}$$

where V_c is the incipient motion velocity of tailings.

$$\frac{V_c}{\sqrt{\gamma_s - \gamma/\gamma g}\ \overline{D}\,(R/D)^{1/6}} = 0.0035\left(\frac{NR^{1/6}}{\sqrt{g}\,n\text{Re}_{vd}}\right)^2 + 1.5. \tag{2}$$

In the formula, N is a constant, usually 11.6; R is the hydraulic radius; $R = ab/2\,(a + b)$, where a and b are the height and width of rectangular pipes; n is roughness; Re_{vd} is the starting Reynolds number of sediment; γ_s is sediment

bulk density; γ is the bulk density of water; D is sediment particle size.

Li [11] and Kandiah [20] obtained the nonlinear relationship between the sediment erosion and relative residual shear stress through the silt scouring test. The physical and chemical characteristic index l was proposed by the dimensionless method, and the formula of sediment scouring rate was established:

$$E = M\left(\frac{\tau_b}{\tau_c} - 1\right)^l. \tag{3}$$

In the formula, E is a sediment erosion rate; τ_b is the flow shear stress; τ_c is the critical starting shear stress of tailings; M is a dimensional scouring constant, with the unit of mm/s, which varies with the sediment type and various physicochemical properties; $\tau_b/\tau_c - 1$ represents the relative residual shear stress; the value of index l is related to the properties of the sediment.

To obtain the incipient motion velocity V_c' of the reinforced tailings particles with different geogrid spacing, eight tailings samples were calculated according to (1). The flow velocity U in the erosion rate test data of the reinforced tailings from Tables 2–5 is used to calculate the relative residual shear stress of reinforced tailings under different geogrid spacing according to (3) $(U^2/V_c^{'2} - 1)$. Finally, the flow velocity U, the incipient motion velocity V_c', the relative residual shear stress τ', and the erosion rate E of the reinforced tailings particles are obtained as listed in Table 6, along with the erosion rate of tailings corresponding to relative residual shear stress under different geogrid spacing.

According to the erosion rate of various reinforced tailings spacings, the erosion constant M and physicochemical property index l in the erosion rate (3) of the reinforced tailings are fitted. The erosion rate curve of the reinforced tailings is plotted, as shown in Figure 8. The abscissa represents the relative residual shear stress under different geogrid spacing, and the ordinate represents the erosion rate of the reinforced tailings.

In the fitting process of the erosion rate formulas of different geogrid spacings, since the geogrid spacing has been considered in τ_c, namely V_c', the erosion constant and physicochemical index in the erosion rate formula will no longer be considered as the functions of geogrid spacing. In summary, the erosion rate formula of the reinforced tailings can be fitted as follows:

TABLE 6: Value of relative residual shear stress τ' and corrosion rate E of reinforced tailings.

Geospacing d(cm)	Sample	U (m/s)	V_c' (m/s)	τ'	E (mm/s)
	1	0.840	0.559	1.001	0.062
	2	0.264	0.187	0.768	0.058
	3	0.264	0.203	0.504	0.048
2.5	4	0.264	0.162	1.356	0.067
	5	0.264	0.160	1.421	0.071
	6	0.264	0.158	1.485	0.075
	7	0.264	0.190	0.718	0.057
	8	0.264	0.192	0.673	0.054
	1	0.840	0.560	0.785	0.052
	2	0.264	0.186	0.585	0.048
	3	0.264	0.201	0.365	0.042
1.7	4	0.264	0.161	1.120	0.053
	5	0.264	0.159	1.194	0.058
	6	0.264	0.160	1.142	0.054
	7	0.264	0.190	0.521	0.044
	8	0.264	0.193	0.474	0.043
	1	0.840	0.561	0.595	0.039
	2	0.264	0.186	0.430	0.038
	3	0.264	0.201	0.226	0.031
1.3	4	0.264	0.162	0.875	0.042
	5	0.264	0.160	0.928	0.048
	6	0.264	0.159	0.957	0.050
	7	0.264	0.191	0.360	0.035
	8	0.264	0.192	0.347	0.033
	1	0.840	0.698	0.450	0.027
	2	0.264	0.234	0.269	0.025
	3	0.264	0.253	0.089	0.015
1.0	4	0.264	0.205	0.653	0.033
	5	0.264	0.199	0.753	0.038
	6	0.264	0.199	0.757	0.042
	7	0.264	0.237	0.238	0.023
	8	0.264	0.243	0.181	0.021

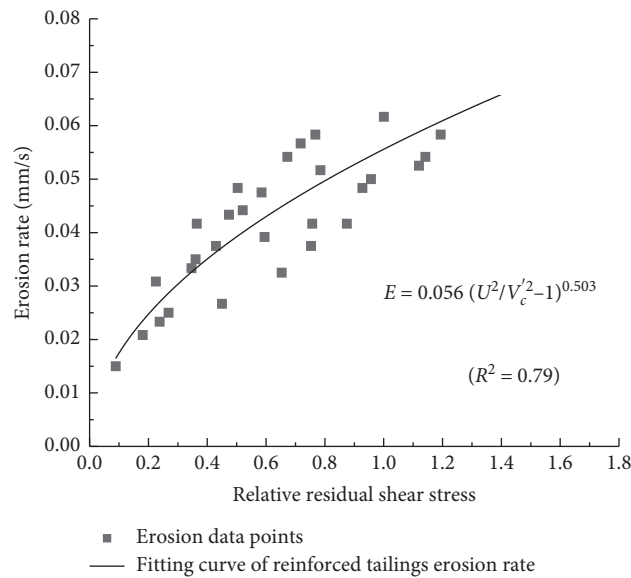$$E = 0.056 \, (U^2/V_c'^2 - 1)^{0.503}$$

$$(R^2 = 0.79)$$

FIGURE 8: Relationship between erosion rate of reinforced tailings and relative residual shear stress.

$$E = 0.056\left(\frac{U^2}{V_c'^2} - 1\right)^{0.503} \left(R^2 = 0.79\right). \quad (4)$$

Equation (4) is a formula for calculating the erosion rate of reinforced tailings selected near the geogrid d_x. However, it is not considered that the actual reinforced tailings pond will collapse in the whole process of overtopping. When establishing a hydraulic erosion rate model for reinforced tailings dam, the formula of reinforced tailings erosion rate needs to be further modified through the overtopping erosion test of the reinforced tailings dam.

4.2. Correction of Collapse Coefficient Based on Overtopping Test.

To modify the formula of erosion rate of the reinforced tailings, the overtopping erosion test of reinforced tailings dam with different geogrid spacing is carried out to obtain the overtopping erosion amount. The experimental value of the erosion amount is compared with the calculated value of (4), and the collapse coefficient is introduced to modify (4). The overtopping erosion test of the reinforced tailings dam adopts the simulation test bench of tailings dam failure designed by the authors, which mainly includes water supply system, tailings dam test groove, and dam failure monitoring system. The test tank is made of acrylic material, with the length, width, and height of 50, 30, and 30 cm, respectively.

Taking into account the size of the test platform, the size of the reinforced tailings dam overtopping erosion test is 48 cm × 30 cm × 24 cm (length × width × height); the slope ratio of the model is 1: 1.5; the slope ratio of the inner slope is 1: 2.0; and the slope top height is 24 cm. In this study, a total of five groups of overtopping dam failure tests of reinforced tailings reservoirs with geogrid spacings of 3.0, 4.0, 4.5, 6.0, and 7.5 cm (i.e. the number of geogrid layers is 6, 5, 4, 3, and 2) are designed. The test illustration of the reinforced tailings dam with the geogrid spacing of 6.0 cm is shown in Figure 9.

① Samples with 15% moisture content are prepared as required and sealed for 12 h

② The layered compaction method is adopted to compact the samples, with the thickness of 6 cm and the compaction degree of 90%

③ The reinforced strip is laid according to the spacing of 3.0, 4.0, 4.5, 6.0, and 7.5 cm, respectively, by using a glass fiber screen window

4.2.1. Steps of Reinforced Tailings Dam Overtopping Erosion Test

① It is standstill after the water injection height of the tailings dam reaches 6 cm through the water supply system, so that the reservoir water infiltrates into the dam body. And water is injected into the reservoir again to keep the water level unchanged; then, the flood dam test is started.

② The color foam balls are put into the tailings dam as a tracking point, and the high-resolution camera is used
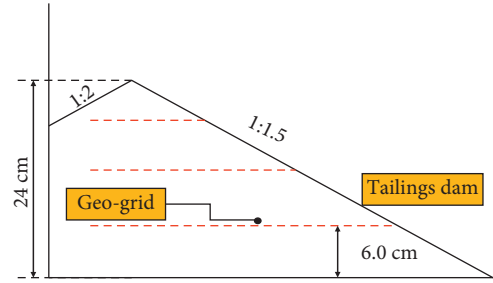

FIGURE 9: Illustration of geogrid arrangement with 6.0 cm spacing.

to capture the motion of the foam ball frame by frame to calculate the overtopping flow velocity.

③ Control flow rate at 22.73 cm³/s for 4 min, collect eroded tailings to sedimentation, and dry and determine their quality.

4.2.2. The Phenomenon of the Overtopping Erosion Test in the Reinforced Tailings Pond.

The erosion failure process of the dam embankment is described as follows: after 4 min overtopping of the reinforced tailings dam, erosion failure with different degrees of gully, width, and depth of breach has appeared on the surface of the dam embankment, as shown in Figure 10.

From Figure 10, it can be seen, in the progressive erosion and failure process of the reinforced tailings dam overtopping, with the decrease of geogrid spacing, the width of gully formed on the surface of the dam body is gradually reduced, and the dam collapses disappear progressively. It can be seen that the geogrid can effectively reduce the erosion and failure of the tailings dam when the flood is overtopping.

4.2.3. Correction of Collapse Coefficient Based on Macro-Overtopping Test.

In the process of overtopping erosion of the reinforced tailings dam, the dam will collapse due to its gravity under the action of water flow. Therefore, the collapse coefficient $K(d)$ is introduced into the erosion rate formula, i.e., (4), of the reinforced tailings, where d is the geogrid spacing. The modified hydraulic erosion rate model of the reinforced tailings dam is

$$E = K(d) \cdot 0.056\left(\frac{U^2}{V_c'^2} - 1\right)^{0.503}. \quad (5)$$

By collecting, drying, and weighing the overtopping erosion amount of the five groups of reinforced tailings dams, the erosion amounts of the reinforced tailings with the geogrid spacing of 3.0, 4.0, 4.5, 6.0, and 7.5 cm are obtained, with the unit of g. Because the unit of the fitting formula of the reinforced tailings erosion rate is mm/s, considering the difference of erosion units, the erosion rate formula is multiplied by the slope area of the dam body to obtain the calculated value of the erosion amount formula in g. In addition, the ratio of erosion amount is the ratio of erosion rate, so the collapse coefficient $K(d)$ can be calculated by the percentage of the overtopping test erosion to calculate
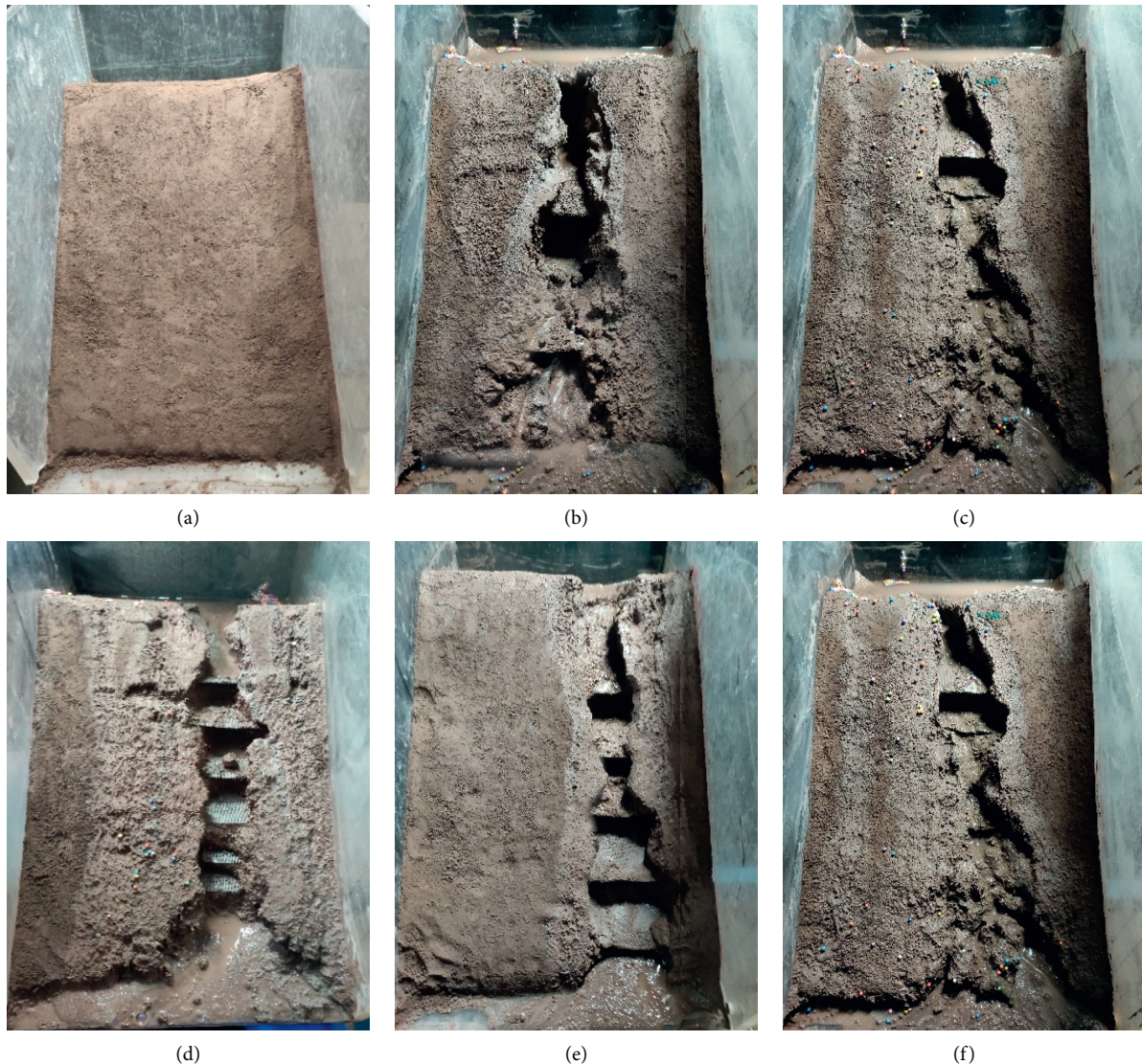
FIGURE 10: Diagrams of reinforced tailings dam failure. (a) Front of reinforced tailings. (b) $d = 7.5$ cm. (c) $d = 6.0$ cm. (d) $d = 4.5$ cm. (e) $d = 4.0$ cm. (f) $d = 3.0$ cm.

erosion from the formula. The values of flow Q, erosion time t, overtopping erosion amount, and collapse coefficient $K(d)$ are listed in Table 7.

Erosion is calculated by the formula of overtopping erosion and erosion rate of the reinforced tailings dam, as shown in Figure 11. It can be seen from Figure 11 that the calculated value of the erosion rate formula of the reinforced tailings is close to that of the reinforced tailings dam when the geogrid spacing is small (the spacing is 3.0~4.5 cm). When the geogrid spacing is larger (spacing >4.5 cm), the erosion caused by the overtopping of the reinforced tailings dam is greater than the calculated value of the erosion rate formula. When the spacing between the reinforcing bars is large, the reinforcing bars' effect only acts near the reinforcing bars of the tailings dam. There is a specific range of influence, so there still will be a small amount of collapse.

From Table 7, it can be seen that the collapse coefficient $K(d)$ is greater than 1 at different geogrid spacings. When the geogrid spacing is less than 4.5 cm, that is, when the geogrid spacing is small, the overtopping erosion of the reinforced tailings reservoir is close to the calculated value of (4). The reinforced tailings pond can be approximately regarded as no collapse occurred during the whole process of overtopping erosion, and the collapse coefficient is close to 1, which is consistent with the phenomenon of the overtopping erosion test of the tailings pond with the geogrid spacing of 3.0~4.5 cm. Figure 12 is fitted by collapse factor $K(d)$ and geogrid distance d.

When the spacing d is less than or equal to 4.5 cm, the collapse coefficient $K(d)$ is close to 1, so when the spacing d is less than 4.5 cm, the collapse coefficient $K(d) = 1$. Linear fitting of the collapse coefficient $K(d)$ and the geogrid spacing d is adopted when geogrid spacing d is greater than

TABLE 7: Erosion amount of the overtopping test of the reinforced tailings pond.

Geospacing d(cm)	Flow rate Q (cm³/s)	Erosion time t (s)	Erosion amount (g)	Formula calculation value (g)	Error percentage	Collapse coefficient $K(d)$
3.0	22.73	240	653	621	4.92	1.05
4.0	22.73	240	731	724	0.98	1.01
4.5	22.73	240	812	802	1.29	1.01
6.0	22.73	240	998	842	15.59	1.18
7.5	22.73	240	1191	843	29.18	1.41
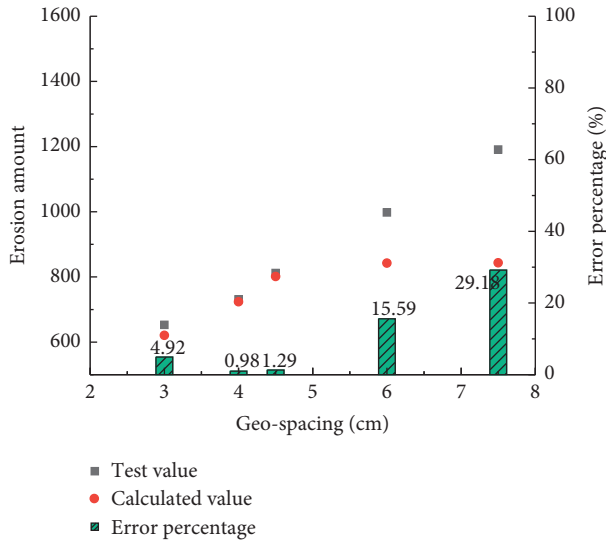
FIGURE 11: Comparison of calculated and measured erosion amounts of reinforced tailings.

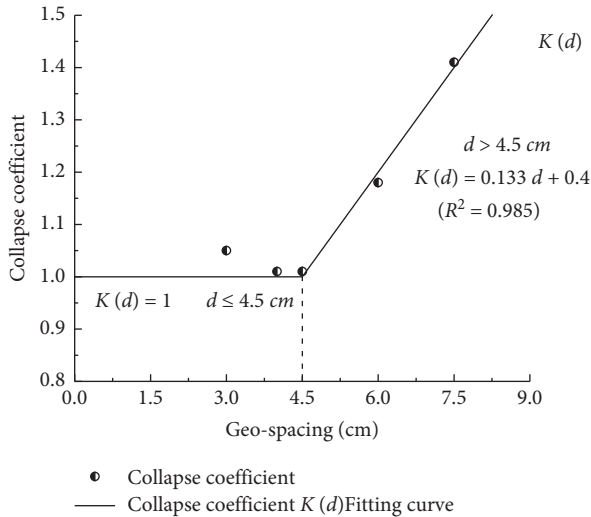
FIGURE 12: Fitting diagrams of collapse coefficient $K(d)$.

4.5 cm, and the collapse coefficient $K(d)$ is expressed by formula (6).

By substituting the collapse coefficient $K(d)$ in (6) into the reinforced tailings erosion rate of (4), the hydraulic erosion rate equation of the reinforced tailings considering collapse factors can be obtained:

$$K(d) = \begin{cases} d \cdot \left(0.133 \, \text{cm}^{-1}\right) + 0.4, & d > 4.5 \, \text{cm} \left(R^2 = 0.985\right) \\ 1, & d \leq 4.5 \, \text{cm} \end{cases},$$

(6)

$$E = \begin{cases} 0.056\,(0.133\,d + 0.4) \cdot \left(\dfrac{U^2}{V_c'^2} - 1\right)^{0.503}, & d > 4.5 \, \text{cm} \\ 0.056\left(\dfrac{U^2}{V_c'^2} - 1\right)^{0.503}, & d \leq 4.5 \, \text{cm} \end{cases}$$

(7)

5. Conclusions

In this paper, the influence of geogrid spacing on the erosion rate of reinforced tailings is analyzed through a series of erosion and overtopping tests. Based on the existing erosion rate formula, the effects of the erosion constant and physicochemical property index on the erosion rate are considered. The following conclusions can be drawn:

(1) The hydraulic erosion test of tailings with different geogrid spacing (1.0, 1.3, 1.7, 2.5 cm) was carried out by self-made reinforced tailings hydraulic erosion test device. It was found that with the decrease of geogrid spacing, the erosion rate of reinforced tailings particles is gradually reduced. The test results show a positive correlation between the reinforcement spacing and erosion rate of tailings.

(2) Through the tailings reinforced erosion test, the erosion test data were obtained. By considering the influence of erosion constant and physicochemical property index on the erosion rate, the formula of reinforced erosion rate was obtained by combining with the erosion rate.

(3) Based on the theory of sediment scouring, the scouring constant M in the erosion rate formula was determined as 0.056 mm/s by the reinforced tailings erosion test. They were considering that there was a certain collapse in the process of overtopping erosion of reinforced tailings dam. Overtopping erosion tests of the tailings dam with different geogrid spacing (3.0, 4.0, 4.5, 6.0, 7.5 cm) were carried out. The collapse coefficient $K(d)$ was introduced into the formula of reinforced tailings erosion rate, and the formula of hydraulic erosion rate of the reinforced tailings dam was established. When the geogrid spacing $d \leq 4.5$ cm, the collapse coefficient $K(d) = 1$.

When the geogrid spacing $d > 4.5$ cm, the collapse coefficient $K(d)$ is linearly related to the geogrid spacing d.

Data Availability

The data used to support the findings of this study are available from the corresponding author upon request.

Conflicts of Interest

The authors declare that there are no conflicts of interest.

Acknowledgments

References

[1] G. M. Yu, C. W. Song, Y. Z. Pan, and L. Li, "Review of new progress in tailings dam safety in foreign research and current state with development trent in China," *Chinese Journal of Rock Mechanics and Engineering*, vol. 33, no. S1, pp. 3238–3248, 2014.

[2] V. S. Quaresma, A. C. Bastos, M. D. Leite, and A. Costa, "The effects of a tailings dam failure on the sedimentation of the eastern Brazilian inner shelf," *Continental Shelf Research*, vol. 205, Article ID 104172, 2020.

[3] X. Zheng, X. H. Xu, and K. L. Xu, "Study on the risk assessment of the tailings dam break," *Procedia Engineering*, vol. 26, pp. 2261–2269, 2011.

[4] J. R. Owen, D. Kemp, É. Lèbre, and K. Svobodova, "Catastrophic tailings dam failures and disaster risk disclosure," *International journal of disaster risk reduction*, vol. 42, Article ID 101361, 2020.

[5] M. Rico, G. Benito, A. R. Salgueiro, A. Díez-Herrero, and H. G. Pereira, "Reported tailings dam failures," *Journal of Hazardous Materials*, vol. 152, no. 2, pp. 846–852, 2008.

[6] X. S. Li, K. Peng, J. Peng, and D. Hou, "Effect of thermal damage on mechanical behavior of a finegrained sandstone," *Arabian Journal of Geosciences*, vol. 14, no. 1212, 2021.

[7] E. Sun, X. Zhang, Z. Li, and Y. Wang, "Tailings dam flood overtopping failure evolution pattern," *Procedia Engineering*, vol. 28, no. 8, pp. 356–362, 2012.

[8] X. Z. Dang, M. S. Gao, L. T. Zhang, X. Wang, and S. Zhang, "Experimental study on the model of flood overtopping and dam break of a tailing pond under different deposit compactness," *Marine Geology Frontiers*, vol. 34, no. 9, pp. 79–84, 2018.

[9] G. J. Wang, Y. J. Tang, C. Du, and X. Kong, "Experimental study on dam break under water level variation in reservoir," *Journal of Sedimentary Research*, vol. 43, no. 4, pp. 67–73, 2018.

[10] X. K. Zhang, E. J. Sun, and Z. X. Li, "Experimental study on evolution law of tailings dam flood overtopping," *China Safety Science Journal*, vol. 21, no. 7, pp. 118–124, 2011.

[11] H. G. Li, *Study on the Influence of Rainfall Factors on Tailings Dam Break and its Safety Warning Technology*, PhD thesis, University Of Science & Technology Beijing, Beijing, China, 2017.

[12] X. Li, *Experimental Study on Rainfall Induced Collapse of Tailings Pond*, Kunming University of Science and Technology, Kunming, China, 2015.

[13] J. B. Zhao, J. Li, X. H. Bai, C. Miao, and J. Zhang, "Influence of particle orientation on the performance of geogrid reinforced ballast," *Advances in Materials Science and Engineering*, vol. 2020, Article ID 6758059, 12 pages, 2020.

[14] J. Zhang, Z. Y. Zhao, and Z. J. Sun, "Study on long-term performance of geogrid-reinforced and pile-supported embankment at bridge approach," *Advances in Materials Science and Engineering*, vol. 2021, Article ID 5567391, 11 pages, 2021.

[15] X. F. Jing, X. Zhou, Y. S. Zhao, K. Liu, C. Ye, and C. Pan, "Study on influence of reinforcement density on overtopping failure of tailings dam," *Journal of Safety Science and Technology*, vol. 12, no. 8, pp. 68–74, 2016.

[16] X. Zhou, *Study on the Over-topping Evolution Law and Disaster Consequences of Reinforcement Tailings Dam*, Chongqing University of Science and Technology, Chongqing, China, 2016.

[17] L. Zhao, C. Huang, and F. Wu, "Effect of microrelief on water erosion and their changes during rainfall," *Earth Surface Processes and Landforms*, vol. 41, no. 5, pp. 579–586, 2015.

[18] J.-L. Briaud, "Case histories in soil and rock erosion: woodrow wilson bridge, brazos river meander, normandy cliffs, and new orleans levees," *Journal of Geotechnical and Geoenvironmental Engineering*, vol. 134, no. 10, pp. 1425–1447, 2008.

[19] Z. Y. Wang and Y. S. Wu, "A preliminary study on sediment-removing capacity and river motion dynamics," *Journal of Hydraulic Engineering*, vol. 3, pp. 6–11, 2002.

[20] A. Kandiah, *Fundamental Aspects of Surface Erosion of Cohesive Soils*, PhD thesis, University of California, Davis, Calif, 1975.

[21] Q. Zhang, Y. Wang, and C. B. Chen, "Experiment on incipient motion and scour features of artificial filling clay," *Advances in Science and Technology of Water Resources*, vol. 32, no. 6, pp. 75–78, 2012.

[22] A. M. Osman and C. R. Thorne, "Riverbank stability analysis. I: theory," *Journal of Hydraulic Engineering*, vol. 114, no. 2, pp. 134–150, 1988.

[23] R. B. Krone, "Effects of bed structure on erosion of cohesive sediments," *Journal of Hydraulic Engineering*, vol. 125, no. 12, pp. 1297–1301, 1999.

[24] L. P. Sanford and J. P.-Y. Maa, "A unified erosion formulation for fine sediments," *Marine Geology*, vol. 179, no. 1-2, pp. 9–23, 2001.

[25] H. G. Li, M. Q. Yuan, and X. Q. Zhang, "Study on Critical motion and erosion of cohesive sediment," *Journal of Waterway and Harbor*, vol. 3, pp. 20–26, 1995.

[26] J. X. Tang, G. Z. Yin, Z. A. Wei et al., "Model test study about fine grained tailings dam of longdu tailings pone," *China Mining Magazine*, vol. 13, no. 1, pp. 54–56, 2004.

[27] Y. L. Zhou and Y. L. Wang, "Forecast of the bridge local scour depth," *Journal of Xi'an Highway University*, vol. 19, no. 4, pp. 48–50, 1999.

[28] K. H. Liu, H. Cai, X. F. Jing et al., "Study on hydraulic incipient motion model of reinforced tailings," *Water*, vol. 13, no. 15, 2021.

[29] H. A. Einstein, "Formulas for the transportation of bed load," *Transactions of the American Society of Civil Engineers*, vol. 107, no. 1, pp. 561–577, 1942.

[30] Å. Sundborg, "The river Klarälven a study of fluvial processes," *Geografiska Annaler*, vol. 38, no. 2-3, pp. 125–316, 1956.

[31] R. A. Kuhnle, "Incipient motion of sand-gravel sediment mixtures," *Journal of Hydraulic Engineering*, vol. 119, no. 12, pp. 1400–1415, 1993.

[32] H. W. Zhang, "A unified formula for incipient velocity of sediment," *Journal of Hydraulic Engineering*, vol. 43, no. 12, pp. 1387–1396, 2012.

[33] B. R. Li, "Calculation method of threshold velocity of sediment," *Journal of Sedimentary Research*, vol. 1, pp. 73–79, 1959.

[34] R. R. Cai, L. H. Zhang, and H. W. Zhang, "Modifications to Li Baoru's sediment incipient velocity formula," *Journal of Hydraulic Engineering*, vol. 50, no. 5, pp. 547–554, 2019.